Available online at www.sciencedirect.com
ScienceDirect
Applied Numerical Mathematics 58 (2008) 1413–1433
APPLIED NUMERICAL MATHEMATICS
www.elsevier.com/locate/apnum

A gauge finite element method for the 2D Navier–Stokes problem

Ph. Caussignac

LCVMM IMB SB EPFL (Station 8), CH-1015 Lausanne, Switzerland

Available online 25 August 2007

Abstract

We set up a gauge finite element formulation of the 2D steady state incompressible Stokes problem. This formulation allows to decouple the two unknowns from the equations and to take account for the boundary conditions in a non-iterative way. A finite element discretization is used to obtain numerical convergence results. The method is then applied to the Navier–Stokes equations for solving the lid-driven cavity problem and comparing different gauges.

Keywords: Finite elements; Gauge formulation; Navier–Stokes equations

1. Introduction

In this paper, we set up a gauge formulation for the incompressible steady-state Stokes problem which will serve as a basis for solving the Navier–Stokes equations. The basic idea is to write the velocity as $\mathbf{u} = \mathbf{v} - \nabla\pi$ and ensuring that $\mathbf{u}$ is divergence-free by the equation $\triangle\pi = \operatorname{div}\mathbf{v}$. For the Stokes problem, our formulation is quite close to the one presented in [10] (see Theorem 2 below). A related velocity decomposition such that $\mathbf{u} = \nabla\phi + \mathbf{curl}\,\psi$ has been studied in Ref. [5], in the context of fluid mechanics but not for the Stokes problem; a finite element method has been developed in which, like in our method, the original boundary conditions require to solve a linear system involving the boundary nodes. Our formulation represents a justification of the above $(\mathbf{v}, \pi)$ decomposition of the velocity; furthermore, we claim that our decoupling method (see Theorem 4 below) is closer to the original formulation, because we do not introduce an extra unknown like in [9], where a pressure has to be computed in the whole domain.

For the Navier–Stokes problem, our decoupling method, together with a semi-explicit linearization scheme and a finite element method, results in solving several but scalar discrete Laplace-like problems with sparse matrices and some small linear systems with the same dense matrix of order of the number of boundary nodes. All matrices involved remain constant during the iterations.

Gauge formulations have various names in the literature: for example impetus-striction [12], velicity [4] or velocity-impulse density formulations [6]; these different methods are well summarized in [16]. Such formulations have been used in the context of Hamiltonian systems, either for the Euler or Navier–Stokes problem [4,12,15]. Numerical schemes for the conservation laws have been presented in [16,6,19] for the Euler equations and in [3,7,14] for the Navier–Stokes problem. Most of the computations use finite difference methods, but in [7] and [14] some finite element discretizations were set up. The convergence of a finite difference time semi-discretization scheme has been

E-mail address: philippe.caussignac@epfl.ch.

0168-9274/$30.00 © 2007 IMACS. Published by Elsevier B.V. All rights reserved.
doi:10.1016/j.apnum.2007.08.002

studied in [19], and also in [13], but for two other schemes. All these methods are designed for time-dependent problems, the time-stepping algorithm being used for decoupling the boundary condition equation which involves both unknowns [19,13]. The only variational formulation we found in the literature, even in the case of finite elements, appears in [14], where interesting error estimates and numerical results have been presented, for a finite element method quite different than ours, and a semi-implicit discretization in time.

The paper is organized as follows. The basic equations, including the different gauges, are presented in Section 2. The Stokes problem is treated in Section 3, where the decoupling method is set up on a variational formulation basis and then discretized with the finite element of lowest order, allowing us to obtain numerical convergence results. Section 4 deals with the Navier–Stokes problem, formulated with the help of a semi-discrete time scheme, in order to allow its formulation and discretization in a way analogous to the Stokes case. The different gauges are then compared at the example of the lid-driven cavity flow. A small conclusion is presented in Section 5. The computation details as well as proofs of theorems are given in three appendices at the end of the paper.

2. The equations

We consider the incompressible steady state Navier–Stokes problem in a bounded convex, simply connected domain $\Omega \subset \mathbb{R}^2$ with smooth or polygonal boundary Γ. The space variable is denoted by $\mathbf{x} = (x, y)$, the scalar curl of $\mathbf{a} = (a_x, a_y)$ is defined by $\operatorname{curl} \mathbf{a} = \partial_x a_y - \partial_y a_x$ and the vector curl by $\mathbf{curl}\, \varphi = (\partial_y \varphi, -\partial_x \varphi)$.

The standard equations for the unknowns $\mathbf{u} = (u_x, u_y) : \Omega \longrightarrow \mathbb{R}^2$ (velocity) and $p : \Omega \longrightarrow \mathbb{R}$ (pressure) read:

$$-\nu \triangle \mathbf{u} + (\mathbf{u} \cdot \nabla)\mathbf{u} + \nabla p = \mathbf{f} \quad \text{in } \Omega, \tag{1}$$

$$\operatorname{div} \mathbf{u} = 0 \quad \text{in } \Omega, \tag{2}$$

$$\mathbf{u} = \mathbf{g} \quad \text{on } \Gamma; \tag{3}$$

the quantity $\nu > 0$ represents the kinematic viscosity and the given data $\mathbf{f} : \Omega \longrightarrow \mathbb{R}^2$ and $\mathbf{g} : \Gamma \longrightarrow \mathbb{R}^2$ are the external force density and the velocity boundary condition.

In a gauge formulation, we introduce new unknowns which results in a problem without the incompressibility condition (2). The formal computations leading to a gauge formulation can be found in Refs. [4] and [15]. We define the “impulse density” $\mathbf{v}$ [16] by setting:

$$\mathbf{u} = \mathbf{v} - \nabla \pi; \tag{4}$$

for satisfying (2), we require that

$$\triangle \pi = \operatorname{div} \mathbf{v}. \tag{5}$$

Taking the curl of (1) yields $\operatorname{curl}(-\nu \triangle \mathbf{v} + \operatorname{curl} \mathbf{v}(-u_y, u_x) - \mathbf{f}) = 0$, which means that there exists Ψ such that $-\nu \triangle \mathbf{v} + \operatorname{curl} \mathbf{v}(-u_y, u_x) - \mathbf{f} = \nabla \Psi$. There are several possible choices of the gauge field Ψ, which is a quadratic function of $\mathbf{u}$ and $\mathbf{v}$ and determines the form of the convection term in the equation for $\mathbf{v}$. A summary of usual gauges for the Euler equations can be found in Ref. [16]; here, we will compare the following gauges.

(1) *The electric gauge* defined by $\Psi = -\frac{1}{2}|\mathbf{u}|^2$, which yields the following equations for $\mathbf{v}$ and p:

$$(\mathbf{u} \cdot \nabla)\mathbf{u} - \nu \triangle \mathbf{v} = \mathbf{f}, \tag{6}$$

$$p = -\nu \triangle \pi. \tag{7}$$

(2) *The zero gauge* for which $\Psi = 0$, giving the equations:

$$\operatorname{curl} \mathbf{v}(-u_y, u_x) - \nu \triangle \mathbf{v} = \mathbf{f}, \tag{8}$$

$$p = -\nu \triangle \pi - \frac{1}{2}|\mathbf{u}|^2. \tag{9}$$

(3) *The geometric gauge* with $\Psi = -\mathbf{u} \cdot \mathbf{v}$, for which we have:

$$(\mathbf{u} \cdot \nabla)\mathbf{v} + (\nabla \mathbf{u})^t \mathbf{v} - \nu \triangle \mathbf{v} = \mathbf{f}, \tag{10}$$

$$p = \mathbf{u} \cdot \nabla \pi - \nu \triangle \pi + \frac{1}{2}|\mathbf{u}|^2, \tag{11}$$

where

$$(\nabla \mathbf{u}) = \begin{pmatrix} \partial_x u_x & \partial_y u_x \\ \partial_x u_y & \partial_y u_y \end{pmatrix}. \tag{12}$$

(4) *The MP gauge*: $\Psi = -\mathbf{u} \cdot \mathbf{v} + \frac{1}{2}|\mathbf{u}|^2$, with the equations:

$$(\mathbf{u} \cdot \nabla)\mathbf{v} + (\nabla \mathbf{u})^t \nabla \pi - \nu \triangle \mathbf{v} = \mathbf{f}, \tag{13}$$

$$p = \mathbf{u} \cdot \nabla \pi - \nu \triangle \pi. \tag{14}$$

(5) *The PiV gauge* defined by $\Psi = -\frac{1}{2}|\mathbf{v}|^2$ for which the equations read:

$$(\mathbf{v} \cdot \nabla)\mathbf{v} + \operatorname{curl} \mathbf{v}\, \mathbf{curl}\, \boldsymbol{\pi} - \nu \triangle \mathbf{v} = \mathbf{f}, \tag{15}$$

$$p = \mathbf{u} \cdot \nabla \pi + \frac{1}{2}|\nabla \pi|^2 - \nu \triangle \pi. \tag{16}$$

We give in Appendix A the derivation of the two equations for the example of the PiV gauge, the procedure for the other gauges being analogous.

The original problem (1)–(3) for the unknowns $(\mathbf{u}, p)$ is replaced in the gauge formulation by equations (5) and one of Eqs. (6), (8), (10), (13) or (15) for the unknowns $(\mathbf{v}, \pi)$ and suitable boundary conditions that we will describe below. The velocity and pressure can be computed afterwards (or during the calculation if needed within an iteration process: the velocity appears in the equation for $\mathbf{v}$ in several gauges), by using (4) and one of Eqs. (7), (9), (11), (14) or (16). Of course, as far as the computation of $(\mathbf{u}, p)$ is concerned, all these gauges are equivalent for the continuous problem; but, the corresponding discrete problems will have different properties of convergence speed and accuracy.

3. The Stokes case

The problem consists in finding $(\mathbf{u}, p) : \Omega \longrightarrow \mathbb{R}^3$ such that

$$-\nu \triangle \mathbf{u} + \nabla p = \mathbf{f} \quad \text{in } \Omega, \tag{17}$$

$$\operatorname{div} \mathbf{u} = 0 \quad \text{in } \Omega, \tag{18}$$

$$\mathbf{u} = \mathbf{g} \quad \text{on } \Gamma. \tag{19}$$

Here, since there is no convection, the only choice of the gauge is $\Psi = 0$ and we get the final equations set for the unknowns $\mathbf{v}$ and π:

$$-\nu \triangle \mathbf{v} = \mathbf{f} \quad \text{in } \Omega, \tag{20}$$

$$\triangle \pi = \operatorname{div} \mathbf{v} \quad \text{in } \Omega, \tag{21}$$

$$\mathbf{v} - \nabla \pi = \mathbf{g} \quad \text{on } \Gamma, \tag{22}$$

the last equation being nothing else but the translation of $\mathbf{u} = \mathbf{g}$ in terms of the gauge variables.

We denote by $\mathbf{t}$ the oriented unit tangent to Γ and by $\mathbf{n}$ the corresponding outside unit normal.[1] Choosing $\pi = 0$ and $\mathbf{v} \cdot \mathbf{t} = \mathbf{g} \cdot \mathbf{t}$ on Γ allows to satisfy the tangential component of the boundary condition. But, there is no way to satisfy the normal component of this condition without coupling $\mathbf{v}$ and π.

Once $(\mathbf{v}, \pi)$ is known, the velocity can be computed from (4) and the pressure from (7).

3.1. Variational formulations, decoupling method

We consider the homogeneous problem, that is the gauge formulation (20)–(22) with $\mathbf{g} = \mathbf{0}$; the space

$$W_0 = \left\{ (\mathbf{v}, \pi) \in H_0^1(\Omega)^3;\ \int_\Omega \nabla \pi \cdot \nabla \pi'\, d\mathbf{x} = -\int_\Omega \pi' \operatorname{div} \mathbf{v}\, d\mathbf{x}\ \forall \pi' \in H^1(\Omega) \right\}, \tag{23}$$

has been already defined in Ref. [10] and yields the following variational formulation (assuming that $\mathbf{f} \in L^2(\Omega)^2$).

[1] For a polygonal domain $\mathbf{t}$ is not defined everywhere and we replace it by an approximation (see below).

Problem 1. Find $(\mathbf{v}, \pi) \in W_0$ such that

$$\int_\Omega \nabla\mathbf{v} \cdot \nabla\mathbf{v}'\, d\mathbf{x} = \int_\Omega \mathbf{f} \cdot \mathbf{v}'\, d\mathbf{x} \quad \forall(\mathbf{v}', \pi') \in W_0. \tag{24}$$

Theorem 2. *Problem* 1 *has a unique solution* $(\mathbf{v}, \pi)$ *and*

$$(\mathbf{u} = \mathbf{v} - \nabla\pi,\ p = -\nu\triangle\pi) \in H_0^1(\Omega)^2 \times L_0^2(\Omega)$$

is the solution of the Stokes problem.

A discretization of the space W_0 is not easy to find; therefore we will set up a decoupling method, which we can formally summarize as follows. First, in order to get rid of the inhomogeneous right-hand side $\mathbf{f}$, we compute $(\mathbf{w}, \rho)$ (see (25) and (26) below) satisfying Eqs. (20), (21), both with homogeneous boundary conditions. Then, for satisfying (22), we want to add to $(\mathbf{w}, \rho)$ the couple $(\mathbf{v}, \pi)$ such that $-\nu\triangle\mathbf{v} = \mathbf{0}$, $\triangle\pi = \operatorname{div}\mathbf{v}$, in Ω, $\mathbf{v}\cdot\mathbf{t} = 0$, $\pi = 0$, $\mathbf{v}\cdot\mathbf{n} - \partial\pi/\partial n = \partial\varrho/\partial n$, on Γ. Due to the special form of the boundary condition $\mathbf{v}\cdot\mathbf{t} = 0$, we need (27) for writing a variational problem for $\mathbf{v}$; this would be easy if we knew $\eta = \mathbf{v}\cdot\mathbf{n}$ on Γ and would result in (29); but since this equation is coupled to (30), we have to find the function η such that $\eta - \partial\pi/\partial n = \partial\varrho/\partial n$ on Γ, as the solution of (33).

The variational formulation for the inhomogeneous part for the solution consists in solving the two problems:

$$\mathbf{w} \in H_0^1(\Omega)^2 \text{ such that } \int_\Omega \nabla\mathbf{w} \cdot \nabla\mathbf{v}'\, d\mathbf{x} = \int_\Omega \mathbf{f} \cdot \mathbf{v}'\, d\mathbf{x} \quad \forall\mathbf{v}' \in H_0^1(\Omega)^2, \tag{25}$$

$$\rho \in H_0^1(\Omega) \text{ such that } \int_\Omega \nabla\varrho \cdot \nabla\pi'\, d\mathbf{x} = -\int_\Omega \pi' \operatorname{div}\mathbf{w}\, d\mathbf{x} \quad \forall\pi' \in H_0^1(\Omega), \tag{26}$$

which both have a unique solution. Notice that (25) is in fact two scalar problems for each component of $\mathbf{w}$.

Remark 3. For dealing with the inhomogeneous problem $\mathbf{g} \neq \mathbf{0}$, one has only to replace (25) by: $\mathbf{w} - \mathbf{v}_g \in H_0^1(\Omega)^2$ such that $\int_\Omega \nabla\mathbf{w} \cdot \nabla\mathbf{v}'\, d\mathbf{x} = \int_\Omega \mathbf{f} \cdot \mathbf{v}' d\mathbf{x}$ with $\mathbf{v}_g \in H^1(\Omega)^2$ an extension of $\mathbf{g}$.

We denote by $\langle .\,, .\rangle$ the duality bracket between $H^{1/2}(\Gamma)$ and $H^{-1/2}(\Gamma)$, by $\gamma\varphi$ the trace of $\varphi \in H^1(\Omega)$, by $\gamma_n\mathbf{v}$ (resp.by $\gamma_t\mathbf{v}$) the normal (resp. tangential) component of the trace of $\mathbf{v} \in H^1(\Omega)^2$ on Γ and by $\partial\gamma_n\varphi$ the extension to $H^2(\Omega)$ of the normal derivative of a function $\varphi \in \mathcal{D}(\overline{\Omega})$.

The decoupling method relies on the following Green formula for $\mathbf{u} \in H^2(\Omega)^2$, $\mathbf{v} \in H^1(\Omega)^2$:

$$-\int_\Omega \mathbf{v} \cdot \triangle\mathbf{u}\, d\mathbf{x} = \int_\Omega (\operatorname{div}\mathbf{u} \operatorname{div}\mathbf{v} + \operatorname{curl}\mathbf{u} \operatorname{curl}\mathbf{v})\, d\mathbf{x} - \langle\gamma_n\mathbf{v}, \gamma \operatorname{div}\mathbf{u}\rangle - \langle\gamma_t\mathbf{v}, \gamma \operatorname{curl}\mathbf{u}\rangle. \tag{27}$$

The space for the impulse density is defined by:

$$V_0 = \{\mathbf{v} \in H^1(\Omega)^2;\ \gamma_t\mathbf{v} = 0\} \tag{28}$$

and can be equipped with the norm $\|\mathbf{v}\|_{V_0} = (\int_\Omega (\operatorname{div}\mathbf{v}^2 + \operatorname{curl}\mathbf{v}^2)\, d\mathbf{x})^{1/2}$, which is equivalent to the H^1-norm (this is a consequence of a particular 2D case of the 3D result of Ref. [1], Lemma 1.5: see Appendix B).

Given $\eta \in H^{-1/2}(\Gamma)$, we compute

$$\mathbf{v}_\eta \in V_0 \text{ such that } \int_\Omega (\operatorname{div}\mathbf{v}_\eta \operatorname{div}\mathbf{v}' + \operatorname{curl}\mathbf{v}_\eta \operatorname{curl}\mathbf{v}')\, d\mathbf{x} = \langle\gamma_n\mathbf{v}', \eta\rangle \quad \forall\mathbf{v}' \in V_0, \tag{29}$$

$$\pi_\eta \in H_0^1(\Omega) \text{ such that } \int_\Omega \nabla\pi_\eta \cdot \nabla\pi'\, d\mathbf{x} = -\int_\Omega \pi' \operatorname{div}\mathbf{v}_\eta\, d\mathbf{x} \quad \forall\pi' \in H_0^1(\Omega). \tag{30}$$

With the help of the mapping $\mathcal{A}: H^{-1/2}(\Gamma) \longrightarrow H^{1/2}(\Gamma)$, $\eta \longmapsto \mathcal{A}\eta = \gamma_n\mathbf{v}_\eta - \partial\gamma_n\pi_\eta$, the solution of the gauge problem will be given by $(\mathbf{v}_\eta, \pi_\eta)$ corresponding to the value of $\eta \in H^{-1/2}(\Gamma)/\mathbb{R}$ such that $\mathcal{A}\eta = \partial\gamma_n\varrho$.

Lemma 4. 1) *There is one and only one solution* $\tilde{\mathbf{v}}_\eta$ *of* (29) *and one has* $\triangle\tilde{\mathbf{v}}_\eta = \mathbf{0}$ *in* $H^{-1}(\Omega)$, $\gamma \operatorname{div} \tilde{\mathbf{v}}_\eta = \eta$ *in* $H^{-1/2}(\Gamma)$.

2) *There is one and only one solution* $\tilde{\pi}_\eta$ *of* (30) *and* $\partial\gamma_n\tilde{\pi}_\eta \in H^{1/2}(\Gamma)$.

Choosing $\mathbf{v}' = \mathbf{v}_{\eta'} - \nabla\pi_{\eta'}$ in (29) allows us to define the bilinear form $a : H^{-1/2}(\Gamma) \times H^{-1/2}(\Gamma) \to \mathbb{R}$ by

$$a(\eta, \eta') = \langle \mathcal{A}\eta', \eta\rangle = \int_\Omega \operatorname{curl}(\mathbf{v}_\eta) \operatorname{curl}(\mathbf{v}_{\eta'})\, d\mathbf{x}; \tag{31}$$

with $\mathbf{v}' = \nabla\rho$ in (29), we obtain the linear form $l : H^{-1/2}(\Gamma) \to \mathbb{R}$ as

$$l(\eta) = \langle \partial\gamma_n\rho, \eta\rangle = \int_\Omega \operatorname{div} \mathbf{v}_\eta \operatorname{div} \mathbf{w}\, d\mathbf{x}. \tag{32}$$

Finally, the variational formulation of our gauge problem consists in finding

$$\eta \in H^{-1/2}(\Gamma)/\mathbb{R} \text{ such that } a(\eta, \eta') = l(\eta') \quad \forall\eta' \in H^{-1/2}(\Gamma)/\mathbb{R}. \tag{33}$$

Theorem 5. *There is one and only one solution* $\tilde{\eta}$ *of* (33). *The pair* $(\mathbf{v}_{\tilde{\eta}} + \mathbf{w}, \pi_{\tilde{\eta}} + \varrho)$ *satisfies Eqs.* (20)–(22) *in the sense of distributions and* $\mathbf{u} = \mathbf{v}_{\tilde{\eta}} + \mathbf{w} - \nabla(\pi_{\tilde{\eta}} + \rho)$, $p = -\nu\triangle(\pi_{\tilde{\eta}} + \varrho)$ *is the solution of the Stokes problem.*

Remark 6. One could argue that decoupling the data $(\mathbf{f}, \mathbf{g})$ by putting them in (25), (26) can be avoided by replacing (29), (30) by an inhomogeneous problem. This is true, but there is an advantage of the method presented here in the case of the discrete version of the Navier–Stokes problem: since the linearization algorithm requires a different right-hand side $\mathbf{f}$ at each iteration, one has only to compute the matrix corresponding to the operator $\mathcal{A}$ once for all. Furthermore, even in the Stokes case, the right-hand side $l(\eta)$ is more difficult to compute when putting the data in the problems for $(\mathbf{v}_\eta, \pi_\eta)$.

3.2. Discretization and numerical results

We shall use finite element spaces for discretizing the gauge problem in its decomposition formulation (25), (26), (29)–(33); these spaces will ensure the C^0-continuity of $\mathbf{v}$ and π. If we use Eq. (4) for computing the velocity, it will not be continuous and hence, we will obtain a non-conforming approximation; furthermore the approximation of the velocity will be a polynomial of one degree less than the approximation of π. In this case, one could choose P_k polynomials ($k \geqslant 1$) for approximating $\mathbf{v}$ and approximate π in P_{k+1}. We prefer, and it is also much easier to code, to choose P_k polynomials for all the unknowns and compute the velocity in another way.

The method of lowest degree is given by P_1 polynomials. Given a usual triangulation τ_h of $\overline{\Omega}$ (we assume the domain to be polygonal or a polygonal approximation of the true domain), we denote by $\mathcal{S}_h$ the set of sides of τ_h and by N_Γ the number of these sides; the corresponding spaces are given by:

$$\begin{aligned}
&X_h = \{\mathbf{v}_h \in C^0(\overline{\Omega})^2; \mathbf{v}_h|_T \in P_1^2\ \forall T \in \tau_h\}, \qquad X_{0h} = X_h \cap H_0^1(\Omega)^2,\\
&V_{0h} = \{\mathbf{v}_h \in X_h; \mathbf{v}_h \cdot \mathbf{t}_h|_{\Gamma\cap\partial T} = 0\ \forall T \in \tau_h \text{ st } \Gamma \cap \partial T \in \mathcal{S}_h\},\\
&\Pi_h = \{\pi_h \in C^0(\overline{\Omega}); \pi_h|_T \in P_1\ \forall T \in \tau_h\}, \qquad \Pi_{0h} = \Pi_h \cap H_0^1(\Omega).
\end{aligned} \tag{34}$$

Finally, we need a finite dimensional space Y_h approximating $H^{-1/2}(\Gamma)$; a natural choice would be to take the space corresponding to the trace of the divergence of functions in V_{0h}. But, we prefer the continuous piecewise P_1 approximation:

$$Y_h = \{g_h \in C^0(\Gamma); g_h|_{\mathcal{S}_h} \in P_1\ \forall\mathcal{S}_h \subset \Gamma\}. \tag{35}$$

At this point, the careful reader can object that the normal and hence the tangent are not defined at the corners of a polygonal domain and hence the essential boundary condition occurring in the definition (34) of V_{0h} can not be satisfied in a standard way by imposing it at the nodes. Such a problem already appeared, but for a boundary condition involving the normal, in the example of Ref. [5]. A way to cure this problem would be to define spaces appropriate to the boundary condition, like in Ref. [18]. We prefer, for simplicity, to approximate the normal (and consequently the tangent) at a corner by the arithmetic mean of the normal of the two adjacent sides; this is the reason of the appearance of $\mathbf{t}_h$ in place of $\mathbf{t}$ in (34).

The discrete approximation of the solution of the gauge problem is obtained in the following way:

(1) Solve (25) with X_{0h} in place of $H_0^1(\Omega)^2$ and $\mathbf{w}_h$ in place of $\mathbf{w}$;
(2) Solve (26) with Π_{0h} in place of $H_0^1(\Omega)$, ρ_h in place of ϱ and $\mathbf{w}_h$ in place of $\mathbf{w}$;
(3) Solve N_Γ times Problem (29) with V_{0h} in place of V_0 and $\mathbf{v}_{\eta_i}$ in place of $\mathbf{v}_\eta$ where $\{\eta_i\}_{1\leqslant i\leqslant N_\Gamma}$ is a basis of Y_h;
(4) Construct the matrix entries $A_{ij}=a(\eta_i,\eta_i)$ with the help of the finite dimensional version of (31) and the vector components $b_i=l(\eta_i)$ from (32) in its finite dimensional form;
(5) Solve the linear system $A\tilde{\eta}=\mathbf{b}$ which is nothing else but the discretization of Problem (33);
(6) Compute

$$\tilde{\mathbf{v}}_h=\sum_{i=1}^{N_\Gamma}\tilde{\eta}_i\mathbf{v}_{\eta_i},\qquad \mathbf{v}_h=\mathbf{w}_h+\tilde{\mathbf{v}}_h,$$

and $\pi_h=\varrho_h+\tilde{\pi}_h$ by solving Problem (30) with Π_{0h} in place of $H_0^1(\Omega)$, $\tilde{\pi}_h$ in place of π_η and $\operatorname{div}\tilde{\mathbf{v}}_h$ in place of $\operatorname{div}\mathbf{v}_\eta$.

For the sake of clarity, let us explain the different points in more details. In the discrete case, the linear operator $\mathcal{A}$ corresponds to a matrix of order N_Γ with entries $a(\eta_i,\eta_j)=\int_\Omega \operatorname{curl}(\mathbf{v}_{\eta_i})\operatorname{curl}(\mathbf{v}_{\eta_j})\,d\mathbf{x}$ which are computed at step (4) using the discrete $\mathbf{v}_{\eta_i}$ calculated at step (3). The linear form l correspond to a vector in $\mathbb{R}^{N_\Gamma}$ with entries $l(\eta_i)=\int_\Omega \operatorname{div}\mathbf{v}_{\eta i}\operatorname{div}\mathbf{w}_h\;d\mathbf{x}$ and is computed in step (4) using $\mathbf{w}_h$ from step (1). Once the linear system has been solved in step (5), the step (6) make use of the linearity in η of (29) for computing $\tilde{\mathbf{v}}_h$; $\tilde{\pi}_h$ can be computed afterwards. The complete approximation $(\mathbf{v}_h,\pi_h)$ requires the knowledge of $(\mathbf{w}_h,\rho_h)$ computed at steps (1) and (2).

So far, we know the approximate solution of the problem in the gauge variables $(\mathbf{v}_h,\pi_h)$ and we have to recover the physical variables. The velocity is computed from the equation $\mathbf{curl}\operatorname{curl}\mathbf{u}=\mathbf{curl}\operatorname{curl}\mathbf{v}$ which yields the variational formulation:

$$\text{find } \mathbf{u}_h-\mathbf{g}_h\in X_{0h} \text{ such that } \int_\Omega \nabla\mathbf{u}_h\cdot\nabla\mathbf{u}'_h\,d\mathbf{x}=\int_\Omega \operatorname{curl}\mathbf{v}_h\operatorname{curl}\mathbf{u}'_h\,d\mathbf{x}\quad \text{for all } \mathbf{u}'_h\in X_{0h}. \tag{36}$$

The pressure is obtained from the equation $p=-\nu\operatorname{div}\mathbf{v}$ and then smoothed to get a continuous P_1 approximation. Thus, we solve:

$$\text{find } p_h\in\Pi_h \text{ such that } \int_\Omega p_h p'_h\,d\mathbf{x}=-\nu\int_\Omega \operatorname{div}\mathbf{v}_h p'_h\,d\mathbf{x}\quad \text{for all } p'_h\in\Pi_h. \tag{37}$$

Remark 7. In our way to compute the velocity, that is by using (36) instead of the discrete version of (4), it is not necessary to compute π_h, nor ϱ_h, if we are interested only in the physical variables.

We want to investigate the convergence rate of our discretization method. The numerical test on the unit square $\Omega=(0,1)\times(0,1)$ is defined by $\nu=1$, the right-hand side by

$$\mathbf{f}=\bigl(2x^2,4x(1-2y)\bigr) \tag{38}$$

and $\mathbf{g}=\mathbf{u}|_\Gamma$ is chosen as the trace of the exact solution

$$\mathbf{u}=\left(x^2\bigl(y-y^2\bigr),-2x\left(\frac{1}{2}y^2-\frac{1}{3}y^3\right)\right). \tag{39}$$

The exact pressure is given by

$$p=2x\bigl(y-y^2\bigr). \tag{40}$$

We denote by $(\mathbf{u}_h,p_h)$ the computed approximations of the velocity and pressure. In Fig. 1, we plot $\|\mathbf{u}-\mathbf{u}_h\|$, in the L_2 (* marks) and H_1(+ marks) norms, versus h^{-1} in log–log scale; assuming the asymptotic behavior $\|\mathbf{u}-\mathbf{u}_h\|\approx Ch^\alpha$

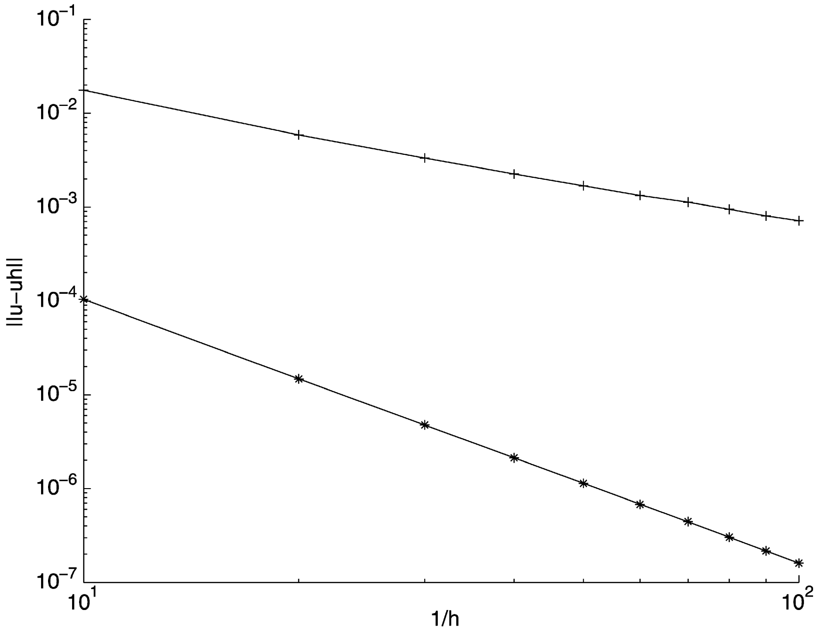

Fig. 1. Velocity error in H_1 and L_2 norm.

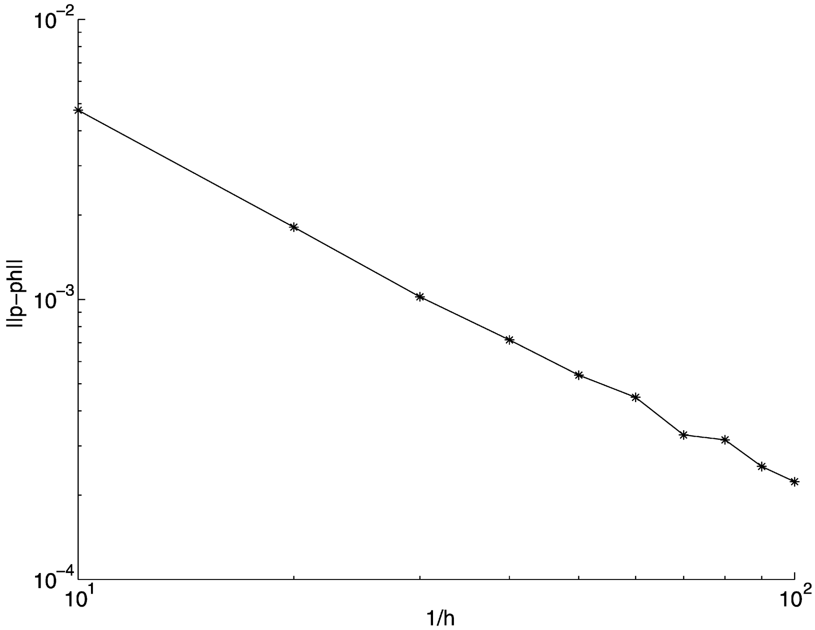

Fig. 2. Pressure error in L_2 norm.

we obtain with the help of a least-square fit: $\alpha \cong 2.81$ for the L_2-norm and $\alpha \cong 1.37$ for the H_1-norm. Compared to usual finite element approximation of the Stokes problem (for example the Crouzeix–Raviart $P_1 \times P_0$ element) for which the theoretical values are $\alpha = 2$ for the L_2-norm and $\alpha = 1$ for the H_1-norm, we see that our method has a very good asymptotic convergence rate.

Fig. 2 contains the plot of $\|p - p_h\|$ in the L_2 norm versus h^{-1}, again in log–log scale; a least-square fit gives here a value of $\alpha \cong 1.32$ which, compared to the theoretical value of $\alpha = 1$ for usual finite elements reveals also a quite good behavior.

To conclude about the Stokes problem, let us recall that its principal difficulty is the incompressibility condition. Usual mixed finite element discretizations of the problem in the primitive variables $(\mathbf{u}, p)$ require interpolation spaces satisfying an inf-sup condition and result in a linear system with a zero diagonal block; solving this system can be avoided by a penalty technique or by finding a "zero-divergence" basis of the interpolation space for the velocity (see [2]). In our method, the finite element spaces are standard ones and the large linear systems (the discrete version of (25), (26), (29) and (30)) are like systems corresponding to a Laplacian; of course, the two latters and specially the largest one (29) has to be solved N_Γ times, which could be quite expensive. But, as pointed out in Remark 6, this is not penalizing for the Navier–Stokes problem, because solving these N_Γ systems shall be done only in the first iteration.

4. The Navier–Stokes case

4.1. Time semi-discrete scheme

Since we want to compare the results obtained with various gauges, we do not set up a very evolved nor optimized linearization scheme for the convective term. The linearization method, already used in [7], is derived from the time-dependent problem corresponding to one of Eqs. (6), (8), (10), (13), (15), and (5) with the boundary condition (22):

$$\mathbf{v}_t + \mathbf{c}(\mathbf{u}, \mathbf{v}, \pi) - \nu \triangle \mathbf{v} = \mathbf{f}, \tag{41}$$

$$\triangle \pi = \operatorname{div} \mathbf{v}, \tag{42}$$

$$(\mathbf{v} - \nabla \pi)|_\Gamma = \mathbf{g}. \tag{43}$$

In Eq. (41), $\mathbf{c}$ denotes the convective term of the corresponding stationary equation for $\mathbf{v}$. The scheme can be viewed as a Crank–Nicolson method for the diffusion term and a Adams–Bashforth method for the convection term. The time semi-discretization with step τ is defined in the following way. Starting from an initial guess $(\mathbf{v}^0, \pi^0)$ (for example the solution of the steady Stokes problem), we look for a sequence $\{(\mathbf{v}^n, \pi^n)\}_{1 \leqslant n}$ of approximations $(\mathbf{v}^n, \pi^n)(\mathbf{x}) \cong (\mathbf{v}, \pi)(\mathbf{x}, n\tau)$ of a solution of (41)–(43). If we set $\alpha = 1/\tau$, we compute $(\mathbf{v}^1, \pi^1)$ from $(\mathbf{v}^0, \pi^0)$, and $(\mathbf{v}^{n+1}, \pi^{n+1})$ from $(\mathbf{v}^n, \pi^n)$ and $(\mathbf{v}^{n-1}, \pi^{n-1})$ for $n \geqslant 2$, by first setting:

$$\mathbf{c}^{3/2}(\mathbf{u}, \mathbf{v}, \pi) = \mathbf{c}\big(\mathbf{u}^0, \mathbf{v}^0, \pi^0\big), \tag{44}$$

$$\mathbf{c}^{n+1/2} = \frac{3}{2}\mathbf{c}\big(\mathbf{u}^n, \mathbf{v}^n, \pi^n\big) - \frac{1}{2}\mathbf{c}\big(\mathbf{u}^{n-1}, \mathbf{v}^{n-1}, \pi^{n-1}\big), \quad n = 2, 3, \ldots, \tag{45}$$

where

$$-\triangle \mathbf{u}^k = \mathbf{curl}\,\mathrm{curl}\,\mathbf{v}^k \quad \text{in } \Omega, \qquad \mathbf{u}^k = \mathbf{g} \quad \text{on } \Gamma. \tag{46}$$

Then, for computing $(\mathbf{v}^{n+1}, \pi^{n+1})$, we solve:

$$\begin{aligned} &\alpha\big(\mathbf{v}^{n+1} - \mathbf{v}^n\big) - \frac{\nu}{2}\triangle \mathbf{v}^{n+1} = \mathbf{f} + \frac{\nu}{2}\triangle \mathbf{v}^n - \mathbf{c}^{n+1/2} \quad \text{in } \Omega,\\ &\triangle \pi^{n+1} = \operatorname{div} \mathbf{v}^{n+1} \quad \text{in } \Omega,\\ &\mathbf{v}^{n+1} - \nabla \pi^{n+1} = \mathbf{g} \quad \text{on } \Gamma. \end{aligned} \tag{47}$$

The last problem is nothing else but a Stokes problem in gauge formulation with an inhomogeneous right-hand side.

4.2. Variational formulations

For solving (47), we use of course the same sort of decoupling as in the Stokes case. For simplifying the notations, we set:

$$\mathbf{v} = \mathbf{v}^{n+1}, \qquad \pi = \pi^{n+1}, \tag{48}$$

$$\mathbf{G} = \alpha \mathbf{v}^n + \mathbf{f} + \frac{\nu}{2}\triangle \mathbf{v}^n - \mathbf{c}^{n+1/2}, \tag{49}$$

and rewrite (47) as:

$$\begin{aligned}
&\alpha\mathbf{v} - \frac{\nu}{2}\triangle\mathbf{v} = \mathbf{G} \quad \text{in } \Omega,\\
&\triangle\pi = \operatorname{div}\mathbf{v} \quad \text{in } \Omega,\\
&\mathbf{v} - \nabla\pi = \mathbf{g} \quad \text{on } \Gamma.
\end{aligned} \tag{50}$$

We then decompose the unknowns in an homogeneous and inhomogeneous part:

$$\mathbf{v} = \mathbf{w} + \tilde{\mathbf{v}}, \qquad \pi = \varrho + \tilde{\pi}, \tag{51}$$

which shall be solutions of the next problems:

$$\begin{aligned}
&\alpha\mathbf{w} - \frac{\nu}{2}\triangle\mathbf{w} = \mathbf{G} \quad \text{in } \Omega,\\
&\mathbf{w} = \mathbf{g} \quad \text{on } \Gamma,
\end{aligned} \tag{52}$$

$$\begin{aligned}
&\triangle\varrho = \operatorname{div}\mathbf{w} \quad \text{in } \Omega,\\
&\varrho = 0 \quad \text{on } \Gamma,
\end{aligned} \tag{53}$$

$$\begin{aligned}
&\alpha\tilde{\mathbf{v}} - \frac{\nu}{2}\triangle\tilde{\mathbf{v}} = \mathbf{0} \quad \text{in } \Omega,\\
&\triangle\tilde{\pi} = \operatorname{div}\tilde{\mathbf{v}} \quad \text{in } \Omega,\\
&\tilde{\pi} = 0, \quad \tilde{\mathbf{v}} - \nabla\tilde{\pi} = \nabla\varrho \quad \text{on } \Gamma.
\end{aligned} \tag{54}$$

Remark 8. It is worthwhile noticing that the homogeneous problem (54) depends on the "time" step only trough the right-hand side term $\nabla\varrho$. Consequently the matrices for solving its discretized counterpart can be built and factorized only once.

The variational formulations of problems (52) and (53) are straightforward and read:

$$\mathbf{w} \in H_0^1(\Omega)^2 \text{ such that } \alpha\int_\Omega \mathbf{w}\cdot\mathbf{v}'\,d\mathbf{x} + \frac{\nu}{2}\int_\Omega \nabla\mathbf{w}\cdot\nabla\mathbf{v}'\,d\mathbf{x} = \int_\Omega \mathbf{G}\cdot\mathbf{v}'\,d\mathbf{x} \quad \forall\mathbf{v}' \in H_0^1(\Omega)^2, \tag{55}$$

$$\varrho \in H_0^1(\Omega) \text{ such that } \int_\Omega \nabla\varrho\cdot\nabla\pi'\,d\mathbf{x} = -\int_\Omega \pi'\operatorname{div}\mathbf{w}\,d\mathbf{x} \quad \forall\pi' \in H_0^1(\Omega). \tag{56}$$

For problem (54), we proceed like in the Stokes case. First, we set $\beta = \alpha/\nu$; given $\eta \in H^{-1/2}(\Gamma)$, let $\mathbf{v}_\eta \in V_0$ be the solution of

$$\beta\int_\Omega \mathbf{v}_\eta\cdot\mathbf{v}'\,d\mathbf{x} + \int_\Omega (\operatorname{div}\mathbf{v}_\eta\operatorname{div}\mathbf{v}' + \operatorname{curl}\mathbf{v}_\eta\operatorname{curl}\mathbf{v}')\,d\mathbf{x} = \langle\gamma_n\mathbf{v}',\eta\rangle \quad \forall\mathbf{v}' \in V_0 \tag{57}$$

and $\pi_\eta \in H_0^1(\Omega)$ such that

$$\int_\Omega \nabla\pi_\eta\cdot\nabla\pi'\,d\mathbf{x} = -\int_\Omega \pi'\operatorname{div}\mathbf{v}_\eta\,d\mathbf{x} \quad \forall\pi' \in H_0^1(\Omega). \tag{58}$$

Then, the solution of problem (54) is given by $(\mathbf{v}_{\tilde{\eta}}, \pi_{\tilde{\eta}})$, with $\tilde{\eta}$ solution of the problem:

$$\eta \in H^{-1/2}(\Gamma)/\mathbb{R} \text{ such that } a_{ns}(\eta,\eta') = l_{ns}(\eta') \quad \forall\eta' \in H^{-1/2}(\Gamma)/\mathbb{R}, \tag{59}$$

where, according to Eqs. (79) and (82) of Appendix C:

$$a_{ns}(\eta,\eta') = \beta\int_\Omega \mathbf{v}_\eta\cdot\mathbf{v}_{\eta'}\,d\mathbf{x} + \int_\Omega \operatorname{curl}\mathbf{v}_\eta\operatorname{curl}\mathbf{v}_{\eta'}\,d\mathbf{x} - \beta\int_\Omega \nabla\pi_\eta\cdot\nabla\pi_{\eta'}\,d\mathbf{x}, \tag{60}$$

$$l_{ns}(\eta) = \int_\Omega \operatorname{div}\mathbf{w}\operatorname{div}\mathbf{v}_\eta\,d\mathbf{x} + \beta\int_\Omega \nabla\pi_\eta\cdot\nabla\varrho\,d\mathbf{x}. \tag{61}$$

With the help of the norm $|\|\mathbf{v}\|| = \sqrt{\beta\|\mathbf{v}\|_{0,\Omega}^2 + \|\mathbf{v}\|_{V_0}^2}$, equivalent to $\|.\|_{V_0}$, one shows, with the same arguments as in the proof of Lemma 11 of Appendix B, that the trace $\gamma\,\mathrm{div}\,\mathbf{v}$ is a linear continuous function from $\{\mathbf{v} \in V_0;\ \triangle\mathbf{v} = \beta\mathbf{v}\}$ to $H^{-1/2}(\Gamma)$. Hence, the four problems (55), (56), (57) and (58) make sense and each has a unique solution. It is easy to show that both the bilinear form a_{ns} and the linear form l_{ns} are continuous; on can furthermore prove (see Appendix C, Lemma 13), that a_{ns} is symmetric positive definite,which indicates that the discretized form of (59) has a unique solution.

4.3. Algorithmic details

We use the same $P1 \times P1$ discretization for $(\mathbf{v}, p)$ as for the Stokes problem. Since we want to solve the Navier–Stokes problem for Reynolds numbers ranging from 1 to 400, that is $1 \geqslant \nu \geqslant 0.0025$, we use a pseudo-continuation method for small viscosities consisting in extrapolating the initial approximation for a given viscosity from the converged approximations of two preceding values with a Newton-chord method. The algorithm for solving the discrete problem at a fixed viscosity splits in two basic steps outlined hereafter. For simplicity, the description is made by referring to the continuous problems, but these ones are replaced by discrete problems in an obvious way, the index h indicating the corresponding discrete variables. In linear algebra operations, we identify these variables with the vector, the component of which are the node values.

- *Iteration* 0
  1. Either compute the first approximation as the solution of the Stokes problem or read the computed solution at the preceding viscosity value, or at the two preceding values to build the first approximation. Compute the velocity from (36) if needed.
  2. Compute and factorize the matrix B_1 for the two scalar Laplace problems (56) and (58). Keep a copy D_1 of the unfactorized matrix.
  3. Compute and factorize the matrix A_1 for the augmented Laplace operator $\alpha\mathbb{I} - \nu\triangle$ corresponding to each component of Problem (55).
  4. Compute the matrix C_1 for the augmented Laplace operator $\alpha\mathbb{I} + \nu\triangle$ for building the first part of each component of the right-hand side of Problem (55) using (49).
  5. Solve N_Γ times the discrete form of Problems (57) and (58) for $\eta = \eta_i$, with $\{\eta_i\}_{1\leqslant i\leqslant N_\Gamma}$ a basis of Y_h. Keep the solutions $(\mathbf{v}_{\eta_i}, \pi_{\eta_i})$ in memory. Build the matrix $A_{ij} = a_{ns}(\eta_i, \eta_j)$.
  6. Compute the matrix D_2 corresponding to the first term of the right-hand side of (61).
- *Iteration* $k > 0$
  For these iterations, we need only to solve linear systems with already factorized matrices and to build right-hand sides by multiplying vectors with existing matrices.
  1. Compute the convective terms for the right-hand sides of (55) according to (49); add to them the contribution from the preceding iteration obtained by multiplying each component of $\mathbf{w}_h$ by the matrix C_1 and add the vector $\mathbf{f}_h$. Solve Problems (55), yielding the new $\mathbf{w}_h$.
  2. Solve Problem (56) for ϱ_h.
  3. Build the vector $b_i = l_{ns}(\eta_i)$ with matrix multiplications $D_2\mathbf{v}_{\eta_i}$, $D_1\pi_{\eta_i}$, followed by dot-products.
  4. Compute the solution of $A\mathbf{x} = \mathbf{b}$; compute $\tilde{\mathbf{v}}_h = \sum_i x_i\mathbf{v}_{\eta_i}$, $\tilde{\pi}_h = \sum_i x_i\pi_{\eta_i}$, $\mathbf{v}_h = \mathbf{w}_h + \tilde{\mathbf{v}}_h$, $\pi_h = \tilde{\pi}_h + \varrho_h$.
  5. Compute $\mathbf{u}_h$ from (36).

4.4. Numerical results

We start our computations by solving the problem, the exact solution of which is given by (39), (40), but of course with the right-hand side

$$\mathbf{f} = \left(2x^2 + x^3y^2\left(1 - \frac{4}{3}y + \frac{3}{2}y^2\right), 4x(1-2y) + x^2y^3\left(1 - \frac{5}{3}y + \frac{3}{2}y^2\right)\right). \tag{62}$$

We observed the following results (with the same notations as in Section 3.2). The L_2-norm $\|\mathbf{u} - \mathbf{u}_h\|$ is almost the same for all gauges: in Table 1 we give these typical results for the geometric gauge (the best one) and the PiV gauge (the worst one).

Table 1
L_2-norm $\|\mathbf{u}-\mathbf{u}_h\|$

h	Geometric	PiV
1/20	0.00461	0.00448
1/40	0.00195	0.00200
1/60	0.00125	0.00135
1/80	0.000985	0.00105
1/100	0.000758	0.000849

Table 2
L_2-norm $\|p-p_h\|$

h	Electric	PiV
1/20	0.00155	0.00163
1/40	0.000937	0.000977
1/60	0.000633	0.000657
1/80	0.000433	0.000497
1/100	0.000319	0.000388

Table 3
H_1-norm $\|\mathbf{u}-\mathbf{u}_h\|$

h	Geometric	Electric	PiV
1/20	0.0155	0.0171	0.0174
1/40	0.0116	0.0130	0.0150
1/60	0.00885	0.0100	0.0152
1/80	0.00714	0.00810	0.0176
1/100	0.00594	0.00674	0.0210

The same behavior occurs for the L_2-norm $\|p-p_h\|$ and is illustrated in Table 2 for the electric gauge (best one) and PiV gauge (worst one again).

For the H_1-norm $\|\mathbf{u}-\mathbf{u}_h\|$ there are significative differences between the gauges; in particular, the PiV gauge appears as not convergent in this norm. Results are presented in Table 3, for the best gauge (Geometric), the middle one (Electric) and the worst one (PiV).

For comparing the different gauges on a physical problem, we choose the well-known lid-driven cavity, defined by $\Omega=(0,1)\times(0,1)$, $\mathbf{f}=\mathbf{0}$ and

$$\mathbf{g}(x,y)=\begin{cases}(1,0), & y=1,\ 0\leqslant x\leqslant 1,\\ \mathbf{0} & \text{on } \Gamma\backslash\{1,0\leqslant x\leqslant 1\}.\end{cases}$$

Of course, the exact solution is not known and our reference solution is the numerical approximation obtained with a spectral finite element code with a very fine uniform mesh built of 513 points in each space direction [11].

We present first results obtained with a uniform 101×101 nodes mesh, which is fine enough for Reynolds numbers less than 100. As usual for this test problem, we consider a cut of u_x at $x=0.5$ and a cut of u_y at $y=0.5$. For Reynolds numbers less than 50, results for all gauges agree very well and are quite close to the reference "exact" solution. For example, both cuts for the PiV gauge at $Re=10$ are compared to the reference solution in Fig. 3. The agreement of all gauges remains at $Re=50$ for the u_x-cut, but there are differences for the u_y-cut. The electric and MP gauge always give the same results.

In Fig. 4(a) we show the two gauges which have the most different behavior for the u_x-cut. In Fig. 5(b), the u_y-cut for three gauges are presented; we notice the typical following feature: the gauge which is qualitatively better in the right-hand part of the diagram (the geometric gauge) is worse in the left-hand part and vice-versa (see the zero gauge).

For getting results for a Reynolds number equal or greater than 100, we switch to a uniform mesh of 161×161 nodes. The effect of convergence is presented if Fig. 5 at the example of the zero gauge.

Results for a Reynolds number of 100 are given in Fig. 6 for the same gauges as in Fig. 4. Again, there is no difference between the MP and electric gauges and we do not plot the last one. The results for the PiV gauge are very

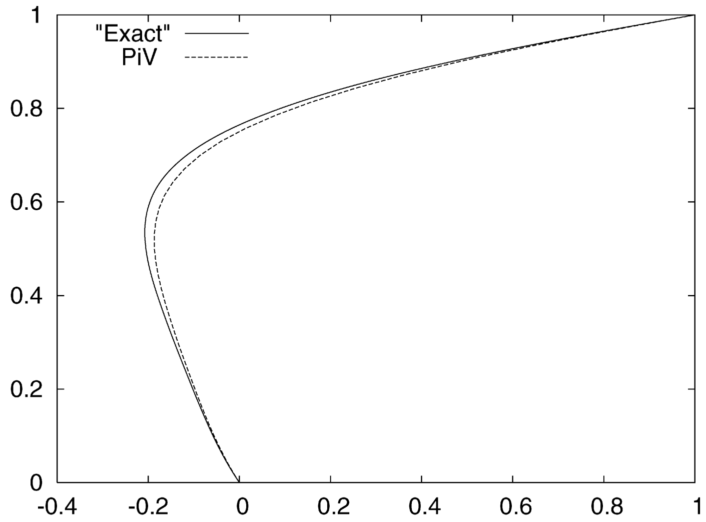

(a) u_x, $Re = 10$

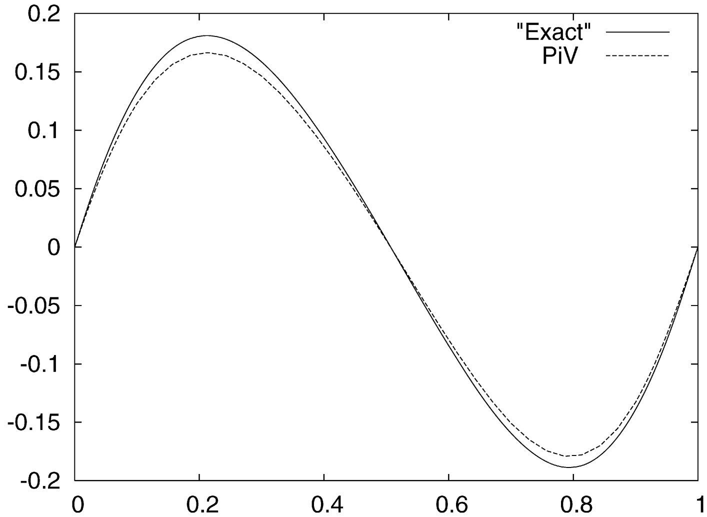

(b) u_y, $Re = 10$

Fig. 3.

bad and not shown. The same typical behavior for the u_y-cut as in Fig. 4 can be noticed, the geometric gauge seeming overall better.

Although our finest mesh is not fine enough for this Reynolds number, the velocity cuts for $Re = 400$ are shown in Fig. 7 for the two best gauges; again, we do not plot results for the MP gauge which are not distinguishable from those for the electric gauge on these diagrams. For the u_x-cut, the geometric gauge has a quite good behavior, but not for the u_y-cut between $x = 0$ and $x = 0.4$.

Finally, the streamlines for Reynold numbers equal to 100 and 400 are presented if Fig. 8, computed on our fine mesh. In Fig. 8(a), we used the electric gauge and in Fig. 8(b) the geometric gauge. The qualitative behavior is in agreement with the usual picture, except near the two bottom corners and principally at the right one.

5. Conclusion

The variational gauge decomposition formulation of the steady state Stokes problem allows to take account for the boundary conditions without an iterative method. Its discretization with the lowest order (P_1) finite element for

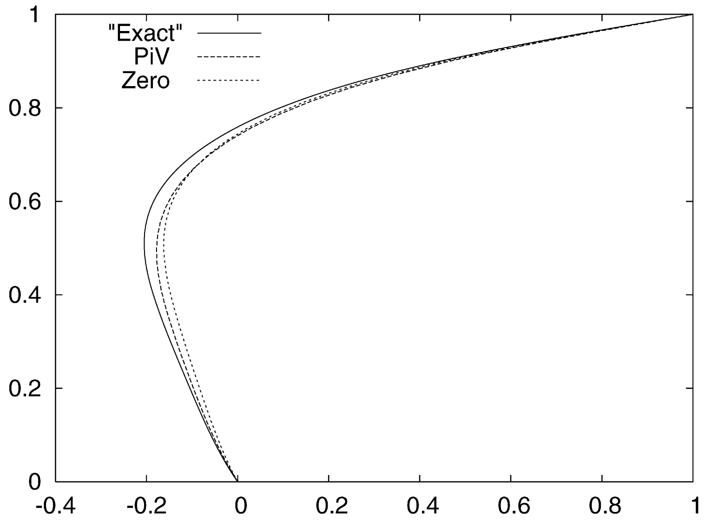

(a) u_x, $Re = 50$

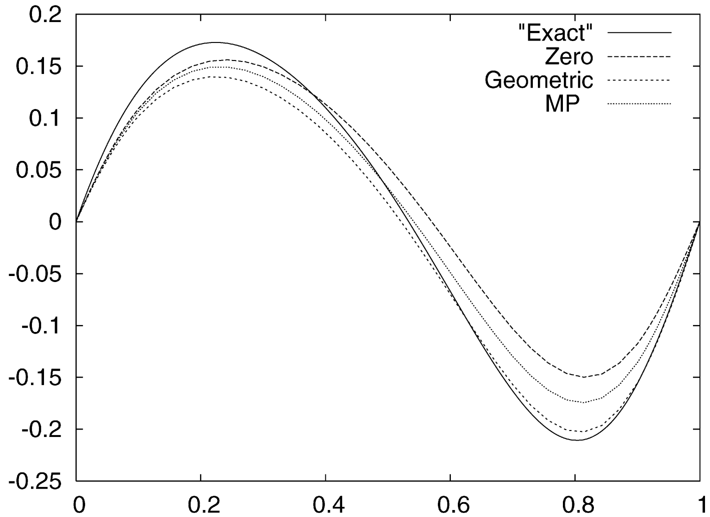

(b) u_y, $Re = 50$

Fig. 4.

both unknowns is easy to implement and exhibits a good numerical convergence behavior. The application of this method, together with a specific linearization scheme, to the Navier–Stokes equations yields to solve only Laplace-like scalar problems with sparse matrices and several dense matrix linear systems of order of the number of boundary nodes. All matrices occurring in the linear systems can be factorized once, before starting the iterations. Numerical comparisons of the different gauges on the driven cavity problem show a good agreement between them and also with the "exact" solution at small Reynold number. At higher Reynolds number, only the electric, MP and geometric gauge give satisfactory results. For all the computations we did, results obtained with the electric and the MP gauge coincide.

Let us mention some future topics which should carry on this work. From the theoretical viewpoint, a priori estimates of the convergence of the discrete Stokes problem in gauge formulation should be proved, as well as stability and convergence of the semi-discrete linearization algorithm for the Navier–Stokes problem. The set up of a more efficient linearization scheme and the optimization of the linear system solving for the Navier–Stokes case shall be undertaken, in order to reach higher Reynold numbers for direct simulations.

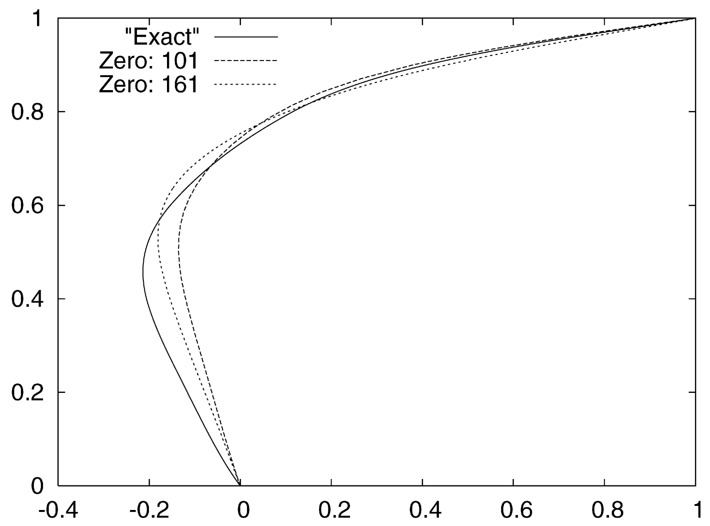

(a) Mesh comparison, $Re = 100$

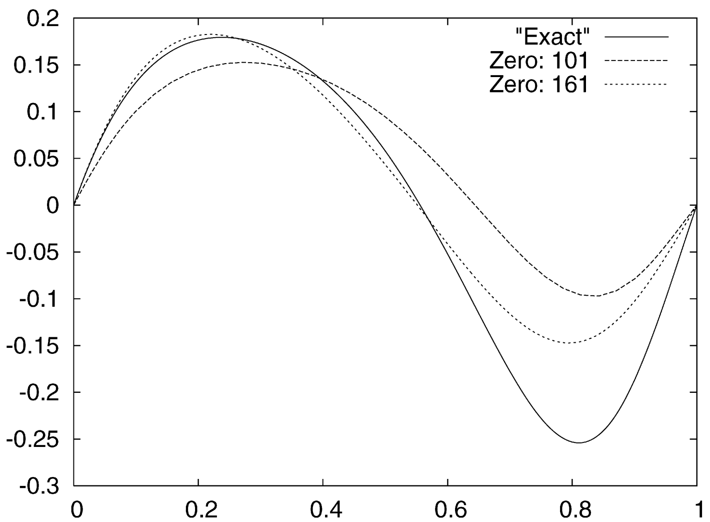

(b) Mesh comparison, $Re = 100$

Fig. 5.

Acknowledgement

The author is very indebted to Emmanuel Leriche for providing him his numerical results for the driven cavity. He also wishes to thank J.H. Maddocks for having pointed to him some gauge methods and R. Touzani for providing to him the library OFELI [17], used to code the method in C++.

Appendix A. Computations for the PiV gauge

In this appendix, we make some formal computations, inspired from Refs. [4] and [15]. We consider the three-dimensional, time-dependent version of Eqs. (1) and (2):

$$\vec{u}_t - \nu \triangle \vec{u} + (\vec{u} \cdot \vec{\nabla})\vec{u} + \vec{\nabla} p = \vec{f}, \tag{63}$$

$$\operatorname{div} \vec{u} = 0. \tag{64}$$

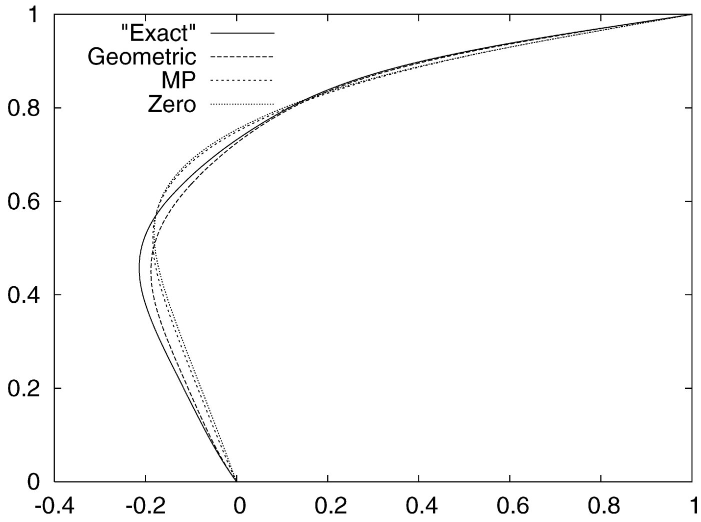

(a) u_x, $Re = 100$

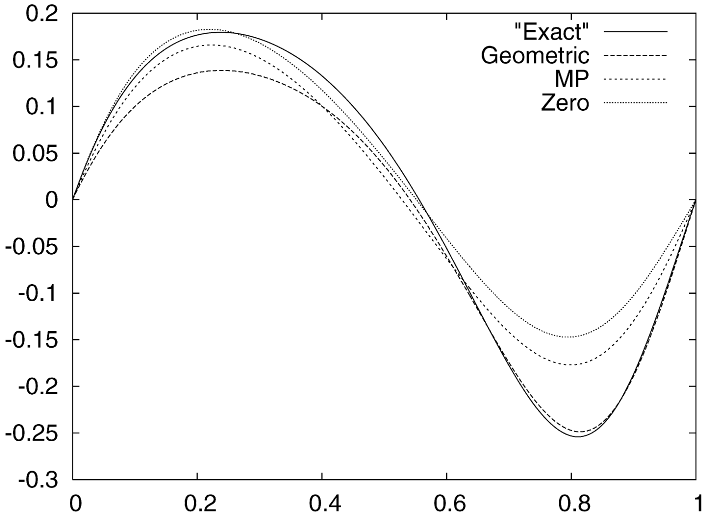

(b) u_y, $Re = 100$

Fig. 6.

We introduce the vorticity $\vec{\omega} = \overrightarrow{\mathrm{curl}}\,\vec{u}$, and, taking the $\overrightarrow{\mathrm{curl}}$ of Eq. (63) yields:

$$\vec{\omega}_t + \overrightarrow{\mathrm{curl}}\big((\vec{u}\cdot\vec{\nabla})\vec{u}\big) - \nu\triangle\vec{\omega} = \overrightarrow{\mathrm{curl}}\,\vec{f}.$$

One has, since $\operatorname{div}\vec{u} = 0$:

$$\overrightarrow{\mathrm{curl}}\big((\vec{u}\cdot\vec{\nabla})\vec{u}\big) = (\vec{u}\cdot\vec{\nabla})\overrightarrow{\mathrm{curl}}\,\vec{u} - (\overrightarrow{\mathrm{curl}}\,\vec{u}\cdot\vec{\nabla})\vec{u},$$

and, using the identity:

$$\overrightarrow{\mathrm{curl}}(\vec{a}\times\vec{b}) = \vec{a}\operatorname{div}\vec{b} - \vec{b}\operatorname{div}\vec{a} + (\vec{b}\cdot\vec{\nabla})\vec{a} - (\vec{a}\cdot\vec{\nabla})\vec{b},$$

yields:

$$\vec{\omega}_t - \overrightarrow{\mathrm{curl}}(\vec{u}\times\vec{\omega}) - \nu\triangle\vec{\omega} = \overrightarrow{\mathrm{curl}}\,\vec{f}. \tag{65}$$

Now, we define the impetus (or velicity) $\vec{v}$ by setting

$$\overrightarrow{\mathrm{curl}}\,\vec{u} = \overrightarrow{\mathrm{curl}}\,\vec{v},$$

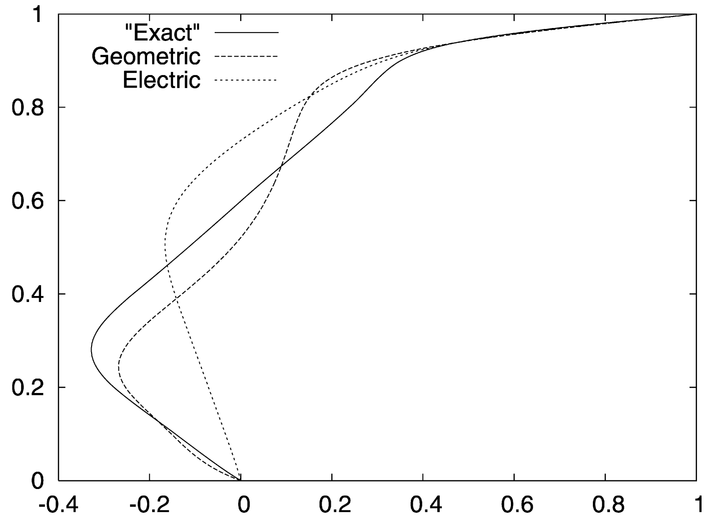

(a) u_x, $Re = 400$

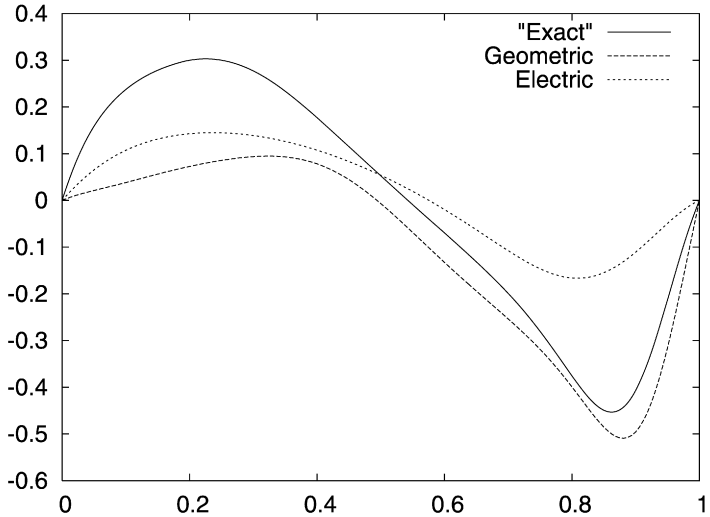

(b) u_y, $Re = 400$

Fig. 7.

and (for simply connected domains) $\vec{v}$ differs from $\vec{u}$ by the gradient of a scalar field π:

$$\vec{u} = \vec{v} - \vec{\nabla}\pi. \tag{66}$$

Using (64), we obtain an equation relating π to $\vec{v}$:

$$\triangle\pi = \operatorname{div}\vec{v}, \tag{67}$$

and since $\vec{\omega} = \overrightarrow{\operatorname{curl}}\,\vec{v}$, Eq. (65) can be written:

$$\overrightarrow{\operatorname{curl}}(\vec{v}_t - \vec{u} \times \overrightarrow{\operatorname{curl}}\,\vec{v} - \nu\triangle\vec{v} - \vec{f}) = \vec{0}.$$

Hence (again for simply connected domains), there exists a scalar field Ψ, the gauge, such that:

$$\vec{v}_t - \vec{u} \times \overrightarrow{\operatorname{curl}}\,\vec{v} - \nu\triangle\vec{v} - \vec{f} = \vec{\nabla}\Psi. \tag{68}$$

We make the explicit choice:

$$\Psi = -\frac{1}{2}|\vec{v}|^2, \tag{69}$$

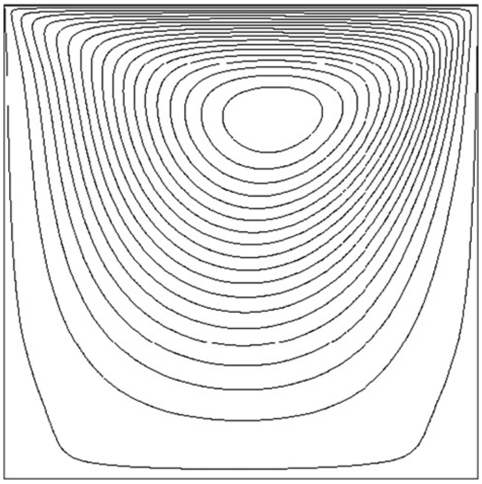

(a) Streamlines, $Re = 100$

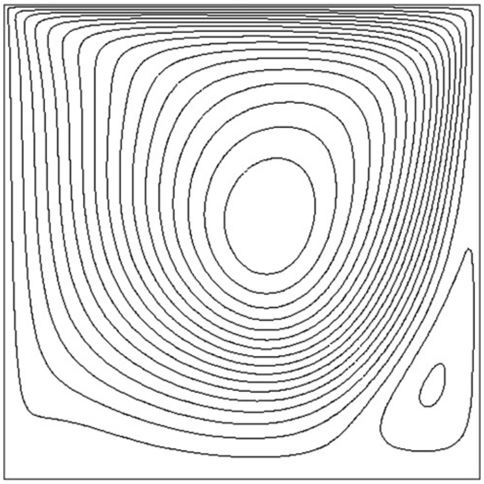

(b) Streamlines, $Re = 400$

Fig. 8.

and using

$$\frac{1}{2}\nabla(|\vec{v}|^2) = \vec{v} \times \overrightarrow{\mathrm{curl}}\,\vec{v} + (\vec{v}\cdot\vec{\nabla})\vec{v},$$

we may rewrite (68) as:

$$\vec{v}_t + (\vec{v}\cdot\vec{\nabla})\vec{v} + \vec{\nabla}\pi \times \overrightarrow{\mathrm{curl}}\,\vec{v} - \nu\triangle\vec{v} = \vec{f}. \tag{70}$$

We want to recover the momentum equation (63) from the latter equation in order to identify the pressure in function of $\vec{v}$ and π. We replace $\vec{v}$ by $\vec{u} + \vec{\nabla}\pi$ in (70) and get

$$\vec{u}_t - \nu\triangle\vec{u} + (\vec{u}\cdot\vec{\nabla})\vec{u} + \vec{\nabla}(\pi_t - \nu\triangle\pi) + (\vec{u}\cdot\vec{\nabla})\vec{\nabla}\pi + (\vec{\nabla}\pi\cdot\vec{\nabla})\vec{u} + \vec{\nabla}\pi \times \overrightarrow{\mathrm{curl}}\,\vec{u} + (\vec{\nabla}\pi\cdot\vec{\nabla})\vec{\nabla}\pi = \vec{f},$$

and hence, the new momentum equation reads

$$\vec{u}_t - \nu\triangle\vec{u} + (\vec{u}\cdot\vec{\nabla})\vec{u} + \vec{\nabla}\left(\pi_t - \nu\triangle\pi + \vec{u}\cdot\vec{\nabla}\pi + \frac{1}{2}|\vec{\nabla}\pi|^2\right) = \vec{f}.$$

We see then that the pressure is given by

$$p = \pi_t - \nu\triangle\pi + \vec{u}\cdot\vec{\nabla}\pi + \frac{1}{2}|\vec{\nabla}\pi|^2. \tag{71}$$

For getting Eqs. (15) and (16), one has just to set $\vec{v} = (\mathbf{v}(\mathbf{x}), 0)$ in (70) and $\vec{u} = (\mathbf{u}(\mathbf{x}), 0)$, $\pi = \pi(\mathbf{x})$ in (71).

Appendix B. Proofs of theorems

Proof of Theorem 2. 1) Since W_0 is a closed subspace of $H_0^1(\Omega)^3$ and the bilinear form $a : W_0 \times W_0 \to \mathbb{R}$, $a(\mathbf{v}, \mathbf{v}') = \nu\int_\Omega \nabla\mathbf{v}\cdot\nabla\mathbf{v}'\,d\mathbf{x}$, is continuous and W_0-elliptic [10], existence and uniqueness result from the Lax–Milgram theorem.

2) Set $\mathbf{u} = \mathbf{v} - \nabla\pi$, $p = -\nu\triangle\pi$. Since $\triangle\pi = \operatorname{div}\mathbf{v}$, $\triangle\pi \in L^2(\Omega)$, which yields $p \in L_0^2(\Omega)$ (since $\int_\Gamma \mathbf{v}\cdot\mathbf{n}\,ds = 0$) and also $\pi \in H^2(\Omega)$. The latter property implies that $\mathbf{u} \in H^1(\Omega)^2$; but, using $\mathbf{v} \in H_0^1(\Omega)^2$, $\pi \in H_0^1(\Omega)$ and $\frac{\partial\pi}{\partial n} = 0$ on Γ, we get $\mathbf{u} \in H_0^1(\Omega)^2$. Using (23), we get in $H^{-1}(\Omega)$: $-\nu\triangle\mathbf{u} = -\nu\triangle(\mathbf{v} - \nabla\pi) = \mathbf{f} - \nabla p$. □

Lemma 9. *Let $\mathbf{v} \in H^1(\Omega)^2$ be such that*

$$\operatorname{div}\mathbf{v} = 0 \quad \textit{and either} \quad \gamma_t\mathbf{v} = 0 \quad \textit{or} \quad \gamma_n\mathbf{v} = 0. \tag{72}$$

Then, one has

$$\|\mathbf{v}\|_{1,\Omega} \leqslant C\|\operatorname{curl}\mathbf{v}\|_{0,\Omega}. \tag{73}$$

Proof. Because of our assumptions about Ω and Γ, this is a particular 2D case of the 3D result of Ref. [1], Lemma 1.5. □

Lemma 10. 1) *V_0 is a closed subspace of $H^1(\Omega)^2$;*
2) *$\|\mathbf{v}\|_{V_0} = (\int_\Omega (\operatorname{div}(\mathbf{v})^2 + \operatorname{curl}(\mathbf{v})^2)\, d\mathbf{x})^{1/2}$ defines a norm on V_0; this norm is equivalent to the usual H^1-norm.*

Proof. 1) Obvious.
2) First, we show that $\|\mathbf{v}\|_{V_0}$ is a norm; since $\|\mathbf{v}\|_{V_0}$ is a semi-norm on $H^1(\Omega)^2$, one has only to prove that $\forall \mathbf{v} \in V_0$ $\|\mathbf{v}\|_{V_0} = 0$ implies $\mathbf{v} = \mathbf{0}$. Let $\mathbf{v} \in V_0$ such that $\|\mathbf{v}\|_{V_0} = 0$; then $\operatorname{div} \mathbf{v} = 0$ and $\int_\Gamma \gamma_n \mathbf{v}\, ds = \int_\Omega \operatorname{div} \mathbf{v}\, d\mathbf{x} = 0$. Then (see [8]) there exists a function $\psi \in H^1(\Omega)$ such that $\mathbf{v} = \operatorname{curl}\psi$. Since $\operatorname{curl} \mathbf{v} = 0$ and $\mathbf{v} \cdot \mathbf{t} = 0$ on Γ, we have $-\triangle\psi = 0$ in $H^{-1}(\Omega)$, $\frac{\partial\psi}{\partial n} = 0$ in $H^{1/2}(\Gamma)$, and consequently ψ is a constant.

Let us prove the equivalence of the norms. Given any $\mathbf{v} \in V_0$, we set $\mathbf{w} = \mathbf{v} - \nabla\varphi$, where $\varphi \in H_0^1(\Omega)$ is such that $\triangle\varphi = \operatorname{div} \mathbf{v}$; then $\mathbf{w}$ satisfies the hypotheses of Lemma 9 with $\gamma_t \mathbf{w} = 0$ and hence $\|\mathbf{w}\|_{1,\Omega} \leqslant C_1 \|\operatorname{curl} \mathbf{v}\|_{0,\Omega}$ because $\operatorname{curl} \mathbf{w} = \operatorname{curl} \mathbf{v}$. Next, we set $\mathbf{u} = (\partial_y\varphi, -\partial_x\varphi)$; one has $\operatorname{div} \mathbf{u} = 0$ and $\mathbf{u}$ satisfies the hypotheses of Lemma 5 with $\gamma_n \mathbf{u} = 0$. Therefore, we have $\|\nabla\varphi\|_{1,\Omega} = \|\mathbf{u}\|_{1,\Omega} \leqslant C_2 \|\operatorname{curl} \mathbf{u}\|_{0,\Omega} = C_2 \|\operatorname{div} \mathbf{v}\|_{0,\Omega}$ since $\operatorname{curl} \mathbf{u} = -\operatorname{div}(\nabla\varphi)$. Finally, one obtains $\|\mathbf{v}\|_{1,\Omega} \leqslant \|\mathbf{w}\|_{1,\Omega} + \|\nabla\varphi\|_{1,\Omega} \leqslant C\|\mathbf{v}\|_{V_0}$.

The inequality $\|\mathbf{v}\|_{V_0} \leqslant C'\|\mathbf{v}\|_{1,\Omega}$ is proven as follows. For $\mathbf{u} \in \mathcal{D}(\overline{\Omega})$, $\mathbf{v} \in V_0$ we have

$$\int_\Omega (\operatorname{div} \mathbf{u} \operatorname{div} \mathbf{v} + \operatorname{curl} \mathbf{u} \operatorname{curl} \mathbf{v})\, d\mathbf{x} = \int_\Omega \nabla\mathbf{u} \cdot \nabla\mathbf{v}\, d\mathbf{x} + \int_\Gamma \gamma_n \mathbf{v} \gamma \operatorname{div} \mathbf{u}\, ds - \int_\Gamma \gamma\mathbf{v} \cdot \partial\gamma_n \mathbf{u}\, ds.$$

By density, this equation remains true for $\mathbf{u} \in H^1(\Omega)^2$, if we replace the boundary integrals by the duality bracket $\langle .,. \rangle$; setting finally $\mathbf{u} = \mathbf{v}$ and using the continuity of the traces gives the result. □

Definition 11. The following space is a closed subspace of V_0:

$$V_{0,\triangle} = \{\mathbf{v} \in V_0;\ \triangle\mathbf{v} = \mathbf{0}\}.$$

Lemma 12. 1) *$\gamma_n : V_0 \longrightarrow H^{1/2}(\Gamma)$ is continuous and onto.*
2) *The mapping $\mathbf{v} \longmapsto \gamma \operatorname{div} \mathbf{v}$ defined from $\mathcal{D}(\overline{\Omega})$ can be extended as a linear continuous function from $V_{0,\triangle}$ to $H^{-1/2}(\Gamma)$.*
3) *One has*

$$\|\gamma \operatorname{div} \mathbf{v}\|_{H^{-1/2}(\Gamma)} \leqslant C\|\operatorname{curl} \mathbf{v}\|_{0,\Omega} \quad \forall \mathbf{v} \in V_{0,\triangle} \text{ such that } \langle 1, \gamma \operatorname{div} \mathbf{v} \rangle = 0.$$

Proof. 1) The continuity follows from the H^1-continuity of each component $\gamma\mathbf{v}$, $\mathbf{v} \in V_0$. Given $\mu \in H^{1/2}(\Gamma)$, let $\varphi \in H^2(\Omega)$ be the unique solution of

$$\triangle^2\varphi = 0 \quad \text{in } H^{-2}(\Omega),$$
$$\gamma\varphi = 0 \quad \text{in } H^{3/2}(\Omega), \qquad \partial\gamma_n\varphi = \mu \quad \text{in } H^{1/2}(\Gamma);$$

then, $\mathbf{v} = \nabla\varphi$ belongs to V_0, $\gamma_n \mathbf{v} = \mu$ and therefore γ_n is onto.
2) Using the Green formula (27), assuming $\mathbf{v} \in V_{0,\triangle}$, we get

$$\int_\Omega (\operatorname{div} \mathbf{v} \operatorname{div} \mathbf{v}' + \operatorname{curl} \mathbf{v} \operatorname{curl} \mathbf{v}')\, d\mathbf{x} = \langle \gamma_n \mathbf{v}', \gamma \operatorname{div} \mathbf{v} \rangle \quad \forall \mathbf{v}' \in V_0.$$

Hence:

$$\left|\langle \gamma_n \mathbf{v}', \gamma \operatorname{div} \mathbf{v} \rangle\right| \leqslant \|\mathbf{v}\|_{V_0} \|\mathbf{v}'\|_{V_0};$$

now, given any $\eta \in H^{1/2}(\Gamma)$, there exits $\mathbf{v}' \in V_0$ such that $\gamma_n \mathbf{v}' = \eta$ and $\|\mathbf{v}'\|_{V_0} \leqslant C\|\eta\|_{H^{1/2}(\Gamma)}$, which implies that $\|\gamma \operatorname{div} \mathbf{v}\|_{H^{-1/2}(\Gamma)} \leqslant C\|\mathbf{v}\|_{V_0}$.

3) Given any $\mu \in H^{1/2}(\Gamma)/\mathbb{R}$, we denote by $(\mathbf{v}_\mu, p_\mu) \in V_0 \times L_0^2(\Omega)$ the solution of the following Stokes problem:

$$-\triangle \mathbf{v}_\mu + \nabla p_\mu = \mathbf{0} \quad \text{in } H^{-1}(\Omega),$$
$$\operatorname{div} \mathbf{v}_\mu = 0 \quad \text{in } L^2(\Omega),$$
$$\gamma_n \mathbf{v}_\mu = \mu.$$

Then, using (27) with $\mathbf{u} = \mathbf{v} \in V_{0,\triangle}$, $\mathbf{v} = \mathbf{v}_\mu$, we obtain

$$\left|\langle \mu, \gamma \operatorname{div} \mathbf{v}\rangle\right| \leqslant \|\operatorname{curl} \mathbf{v}\|_{0,\Omega} \|\mathbf{v}_\mu\|_{1,\Omega} \leqslant C \|\operatorname{curl} \mathbf{v}\|_{0,\Omega} \|\mu\|_{H^{1/2}(\Gamma)}$$

which implies the result. □

Proof of Lemma 4. 1) The bilinear form $\tilde{a}(\mathbf{u}, \mathbf{v}) = \int_\Omega (\operatorname{div} \mathbf{u} \operatorname{div} \mathbf{v} + \operatorname{curl} \mathbf{u} \operatorname{curl} \mathbf{v})\, d\mathbf{x}$ is continuous on V_0 and V_0-elliptic by Lemma 10. Consider the linear form $\mathbf{v} \in V_0 \longmapsto \langle \gamma_n \mathbf{v}, \eta\rangle \in \mathbb{R}$; one has $|\langle \gamma_n \mathbf{v}, \eta\rangle| \leqslant \|\gamma_n \mathbf{v}\|_{H^{1/2}(\Gamma)} \times \|\eta\|_{H^{-1/2}(\Gamma)} \leqslant C(\eta)\|\mathbf{v}\|_{H^1(\Omega)^2} \leqslant C(\eta)\overline{C}\|\mathbf{v}\|_{V_0}$ (the last two inequalities are obtained respectively by Lemma 10, point 1), and Lemma 10, point 2)) and consequently this form is continuous. Then, the Lax–Milgram theorem ensures existence and uniqueness for the problem defined by (29).Using test-functions $\mathbf{v}' \in \mathcal{D}(\Omega)$ in (29) implies that the solution $\tilde{\mathbf{v}}_\eta$ satisfies $-\triangle \tilde{\mathbf{v}}_\eta = 0$ in the sense of distributions and consequently $\tilde{\mathbf{v}}_\eta \in H^2(\Omega)$; then, the Green formula (27) yields

$$\int_\Omega (\operatorname{div} \tilde{\mathbf{v}}_\eta \operatorname{div} \mathbf{v}' + \operatorname{curl} \tilde{\mathbf{v}}_\eta \operatorname{curl} \mathbf{v}')\, dx = \langle \gamma_n \mathbf{v}', \gamma \operatorname{div} \tilde{\mathbf{v}}_\eta\rangle \quad \forall \mathbf{v}' \in V_0.$$

Subtracting the last equation to (29) gives

$$\langle \gamma_n \mathbf{v}', \gamma \operatorname{div} \tilde{\mathbf{v}}_\eta - \eta\rangle = 0 \quad \forall \mathbf{v}' \in V_0;$$

since γ_n is onto $H^{1/2}(\Gamma)$, we have $\langle \mu', \gamma \operatorname{div} \tilde{\mathbf{v}}_\eta - \eta\rangle = 0\ \forall \mu' \in H^{1/2}(\Gamma)$.

2) Existence and uniqueness follow from the Lax–Milgram theorem in $H_0^1(\Omega)$. Since $\triangle \tilde{\pi}_\eta = \operatorname{div} \tilde{\mathbf{v}}_\eta \in L^2(\Omega)$, we have $\tilde{\pi}_\eta \in H^2(\Omega)$ and therefore $\partial\gamma_n \tilde{\pi}_\eta \in H^{1/2}(\Gamma)$. □

Proposition 13. *The linear form $l(.)$ (32) is continuous. The bilinear form $a(.,.)$ (31) is continuous and $H^{-1/2}(\Gamma)/\mathbb{R}$-elliptic.*

Proof. From (32), $|l(\eta)| \leqslant \|\operatorname{div} \mathbf{w}\|_{0,\Omega} \|\operatorname{div} \mathbf{v}_\eta\|_{0,\Omega} \leqslant C\|\mathbf{v}_\eta\|_{V_0}$; with the help of (29) with $v' = \mathbf{v}_\eta$ we get

$$\|\mathbf{v}_\eta\|_{V_0}^2 \leqslant \|\gamma_n \mathbf{v}_\eta\|_{H^{1/2}(\Gamma)} \|\eta\|_{H^{-1/2}(\Gamma)} \leqslant C\|\mathbf{v}_\eta\|_{1,\Omega} \|\eta\|_{H^{-1/2}(\Gamma)} \leqslant C'\|\mathbf{v}_\eta\|_{V_0} \|\eta\|_{H^{-1/2}(\Gamma)}$$

and therefore $|l(\eta)| \leqslant K\|\eta\|_{H^{-1/2}(\Gamma)}$. The inequality $|a(\eta, \eta')| \leqslant \|\mathbf{v}_\eta\|_{V_0} \|\mathbf{v}_{\eta'}\|_{V_0}$ implies, with the same arguments, the continuity $a(.,.)$. Furthermore , the form $a(.,.)$ is $H^{-1/2}(\Gamma)/\mathbb{R}$-coercive thanks to Lemma 12, part 3). □

Proof of Theorem 5. Existence and uniqueness follow from the Lax–Milgram theorem and one checks easily the other affirmations. □

Appendix C. The forms *a* and *l* in the Navier–Stokes case

We set $\beta = 2\alpha/\nu$; let $\mathbf{v}_\eta$ and π_η be the unique solutions of (57) and (58). We want to compute

$$a_{ns}(\eta, \eta') = \langle A\eta', \eta\rangle = \langle \gamma_n \mathbf{v}_{\eta'} - \partial\gamma_n \pi_{\eta'}, \eta\rangle. \tag{74}$$

Using the relationship $\triangle \pi_{\eta'} = \operatorname{div} \mathbf{v}_{\eta'}$ in $H^{-2}(\Omega)$, we get

$$\int_\Omega \operatorname{div} \mathbf{v}_{\eta'} \operatorname{div} \mathbf{v}_\eta\, d\mathbf{x} = \int_\Omega \operatorname{div} \mathbf{v}_\eta \triangle \pi_{\eta'}\, d\mathbf{x} = \langle \partial\gamma_n \pi_{\eta'}, \eta\rangle - \int_\Omega \nabla \operatorname{div} \mathbf{v}_\eta \cdot \nabla \pi_{\eta'}\, d\mathbf{x}; \tag{75}$$

furthermore, in $H^{-2}(\Omega)$

$$\nabla \operatorname{div} \mathbf{v}_\eta = \triangle \mathbf{v}_\eta + \mathbf{curl} \operatorname{curl} \mathbf{v}_\eta = \beta \mathbf{v}_\eta + \mathbf{curl} \operatorname{curl} \mathbf{v}_\eta, \tag{76}$$

the last equality being obtained by using (57) in the sense of distributions. The integral $\int_\Omega \mathbf{curl}\,\mathrm{curl}\,\mathbf{v}_\eta \cdot \nabla\pi_{\eta'}\,d\mathbf{x}$ vanishes and

$$\int_\Omega \mathbf{v}_\eta \cdot \nabla\pi_{\eta'}\,d\mathbf{x} = -\int_\Omega \mathrm{div}\,\mathbf{v}_\eta \pi_{\eta'}\,d\mathbf{x} = \int_\Omega \nabla\pi_\eta \cdot \nabla\pi_{\eta'}\,d\mathbf{x}. \tag{77}$$

Finally, Eqs. (75), (76) and (77) imply that

$$\langle \partial\gamma_n \pi_{\eta'}, \eta\rangle = \int_\Omega \mathrm{div}\,\mathbf{v}_{\eta'}\,\mathrm{div}\,\mathbf{v}_\eta\,d\mathbf{x} + \beta\int_\Omega \nabla\pi_\eta \cdot \nabla\pi_{\eta'}\,d\mathbf{x}. \tag{78}$$

If we set $\mathbf{v}' = \mathbf{v}_{\eta'}$ in (57), we obtain:

$$\langle \gamma_n \mathbf{v}_{\eta'}, \eta\rangle = \beta\int_\Omega \mathbf{v}_\eta \cdot \mathbf{v}_{\eta'}\,d\mathbf{x} + \int_\Omega (\mathrm{div}\,\mathbf{v}_\eta\,\mathrm{div}\,\mathbf{v}_{\eta'} + \mathrm{curl}\,\mathbf{v}_\eta\,\mathrm{curl}\,\mathbf{v}_{\eta'})\,d\mathbf{x},$$

and finally, from (74) and (78):

$$a_{ns}(\eta, \eta') = \beta\int_\Omega \mathbf{v}_\eta \cdot \mathbf{v}_{\eta'}\,d\mathbf{x} + \int_\Omega \mathrm{curl}\,\mathbf{v}_\eta\,\mathrm{curl}\,\mathbf{v}_{\eta'}\,d\mathbf{x} - \beta\int_\Omega \nabla\pi_\eta \cdot \nabla\pi_{\eta'}\,d\mathbf{x}. \tag{79}$$

The last equation shows that a is symmetric.

From Eq. (58) with $\pi' = \pi_\eta$, we get after an integration by parts:

$$\int_\Omega |\nabla\pi_\eta|^2\,d\mathbf{x} = \int_\Omega \mathbf{v}_\eta \cdot \nabla\pi_\eta\,d\mathbf{x},$$

which implies that $\|\nabla\pi_\eta\|_{0,\Omega} \leqslant \|\mathbf{v}_\eta\|_{0,\Omega}$; hence, from (79), we obtain:

$$a_{ns}(\eta, \eta) \geqslant \|\,\mathrm{curl}\,\mathbf{v}_\eta\|^2_{0,\Omega}. \tag{80}$$

Since $\triangle\mathbf{v}_\eta = \beta\mathbf{v}_\eta$, $\mathbf{v}_\eta \in H^2(\Omega)^2$ and even in $C^\infty(\Omega)^2$. Now, assume that η is such that $a_{ns}(\eta,\eta) = 0$; then there exits φ_η such that $\mathbf{v}_\eta = \nabla\varphi_\eta$. Since $\triangle\mathbf{v}_\eta = \beta\mathbf{v}_\eta$, one has

$$\nabla(\beta\varphi_\eta - \triangle\varphi_\eta) = \mathbf{0}$$

and hence $\beta\varphi_\eta - \triangle\varphi_\eta$ is a constant. Since $\mathbf{v}_\eta \in V_0$, $\gamma\varphi_\eta$ is a constant and hence, by continuity, $\gamma\triangle\varphi_\eta = \gamma\,\mathrm{div}\,\mathbf{v}_\eta = \eta$ is also a constant. We then have proved the following result.

Lemma 14. *The bilinear form $a(\cdot,\cdot)$ is symmetric and positive definite on $H^{-1/2}(\Gamma)/\mathbb{R}$.*

The linear form for the right-hand side is defined by:

$$l_{ns}(\eta) = \langle \partial\gamma_n \varrho, \eta\rangle \tag{81}$$

and is computed in a way completely analogous to the arguments leading to (78). The result is

$$l_{ns}(\eta) = \int_\Omega \mathrm{div}\,\mathbf{w}\,\mathrm{div}\,\mathbf{v}_\eta\,d\mathbf{x} + \beta\int_\Omega \nabla\pi_\eta \cdot \nabla\rho\,d\mathbf{x}. \tag{82}$$

References

[1] C. Bègue, C. Concat, F. Murat, O. Pironneau, Les équations de Stokes et de Navier–Stokes avec des conditions aux limites sur la pression, in: H. Brezis, J.-L. Lions (Eds.), Nonlinear Partial Differential Equations and their Applications, Collège de France Seminar, vol. IX, Longman, New York, 1988.

[2] F. Brezzi, M. Fortin, Mixed and Hybrid Finite Element Methods, Springer, Berlin, 1991.

[3] D.L. Brown, R. Cortez, M.L. Minion, Accurate projection method for the incompressible Navier–Stokes equations, J. Comp. Phys. 168 (2001) 464–499.

[4] T.F. Buttke, Velicity methods: Lagrangian numerical methods which preserve the Hamiltonian structure for incompressible flow, in: J.T. Beale, G.H. Cottet, S. Huberson (Eds.), Vortex Flows and Related Numerical Methods, NATO Adv. Sci Inst. Ser. C. Math. Phys. Sci, vol. 35, Kluwer, Dordrecht, 1993.
[5] F. El DabaGhi, O. Pironneau, Stream vectors in three dimensional aerodynamics, Numer. Math. 48 (1986) 561–589.
[6] W. E, J.-G. Liu, Finite difference schemes for incompressible flows in the velocity-impulse density formulation, J. Comp. Phys. 130 (1997) 67–76.
[7] W. E, J.-G. Liu, Gauge finite element method for incompressible flows, Int. J. Numer. Meth. Fluids 34 (2000) 701–710.
[8] V. Girault, P.A. Raviart, Finite Element Approximations of the Navier–Stokes Equations, Lecture Notes in Mathematics, vol. 749, Springer, Berlin, 1979.
[9] R. Glowinski, O. Pironneau, Approximation par éléments finis mixtes du problème de Stokes en formulation vitesse-pression. Résolution des problèmes approchés, C. R. Acad. Sci. Paris Série A 286 (1978) 225–228.
[10] R. Glowinski, O. Pironneau, On a mixed finite element approximation of the Stokes problem, Numer. Math. 33 (1979) 397–424.
[11] E. Leriche, Direct numerical simulation of lid-driven cavity flow by a Chebyshev spectral method, PhD Thesis no 1932, Ecole Polytechnique Fédérale de Lausanne, 1999.
[12] J.H. Maddocks, R.L. Pego, An unconstrained Hamiltonian formulation for incompressible fluid flow, Commun. Math. Phys. 170 (1995) 207–217.
[13] R.H. Nochetto, J.-H. Pyo, Error estimates for semi-discrete gauge methods for the Navier–Stokes equations, Math. Comput. 74 (2004) 521–542.
[14] R.H. Nochetto, J.-H. Pyo, The Gauge–Uzawa finite element method part I: The Navier–Stokes equations, SIAM J. Numer. Anal. 43 (2005) 1043–1068.
[15] M.C. Recchioni, G. Russo, Hamilton-based numerical methods for a fluid–membrane interaction in two or three dimensions, SIAM J. Comput. 19 (1998) 861–892.
[16] G. Russo, P. Smereka, Impulse formulation of the Euler equations: general properties and numerical methods, J. Fluid Mech. 391 (1999) 189–209.
[17] R. Touzani, OFELI: An object finite element library, URL: http://ofeli.sourceforge.net.
[18] R. Verfürth, Mixed finite element approximation of the vector potential, Numer. Math. 50 (1987) 685–695.
[19] C. Wang, J.-G. Liu, Convergence of gauge method for incompressible flow, Math. Comp. 232 (2000) 1385–1407.